

# Mechanistic Insights into the Regioselective Defluorofunctionalization of Trifluoromethylanilines via Photocatalytic SET: A Combined Experimental and Computational Study

Ting Long,<sup>‡</sup> Kazuumi Fujioka,<sup>‡</sup> Yahui Wang,<sup>‡</sup> Qixin Zhou, Liejin Zhou,<sup>\*</sup> Rui Sun,<sup>\*</sup> and Zuxiao Zhang<sup>\*</sup>



Cite This: *Org. Lett.* 2025, 27, 12951–12956



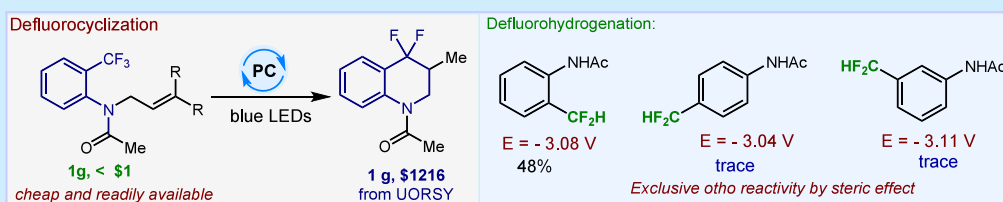
Read Online

ACCESS |

Metrics & More

Article Recommendations

Supporting Information



**ABSTRACT:** We report a photocatalytic method for the selective defluorofunctionalization of trifluoromethylanilines, enabling the synthesis of structurally diverse difluoromethylene-containing aza-heterocycles with broad functional group tolerance. A wide range of alkenes—including di-, mono-, and cyclic olefins—undergo efficient intramolecular cyclization to furnish complex tricyclic scaffolds. Mechanistic investigations, supported by experimental and computational studies, reveal that the observed regioselectivity in defluorohydrogenation is governed primarily by steric effects. This work expands the toolkit for C–F bond activation and offers valuable insights into the design of fluorinated scaffolds for pharmaceutical and materials applications.

Nitrogen-containing heterocycles are foundational motifs in pharmaceuticals and agrochemicals (Figure 1a).<sup>1</sup> Compounds such as oxamniquine, tolvaptan, and argatroban exemplify the therapeutic relevance of these scaffolds.<sup>2–4</sup> In parallel, the incorporation of fluorinated groups—particularly the difluoromethylene (–CF<sub>2</sub>–) unit—has become increasingly important in drug design due to its unique ability to modulate lipophilicity, metabolic stability, and 3D molecular architecture.<sup>5,6</sup> The selective integration of –CF<sub>2</sub>– groups into aza-heterocycles thus presents a valuable yet underexplored synthetic opportunity. A direct and appealing approach involves the selective defluorofunctionalization of trifluoromethyl groups.<sup>7</sup> Traditional methods for C–F bond activation, such as electrochemical reduction,<sup>8</sup> low-valent metal systems,<sup>9</sup> or frustrated Lewis pairs,<sup>10</sup> often suffer from poor selectivity due to the high bond dissociation energy of C(sp<sup>3</sup>)–F bonds (~481 kJ/mol).<sup>11</sup> In response, pioneering work by König, Jui, Gouverneur, and others<sup>12–15</sup> has shown that photoredox catalysis enables efficient generation of difluoromethyl radicals from trifluoromethylarenes under mild conditions.

Among these, Shang's development of *o*-phosphinophenolates represents a key advance in organophotocatalysis.<sup>16</sup> These metal-free, anionic catalysts exhibit exceptional reducing power, enabling selective C–F bond cleavage across a wide range of trifluoromethyl substrates. Mechanistic studies further revealed that the phosphino substituent promotes intersystem crossing and enhances photocatalytic efficiency.<sup>16a</sup> Related

work has demonstrated that other anionic organocatalysts such as BINOLates can also achieve potent reductive activation of challenging substrates like PhCF<sub>3</sub>.<sup>17</sup> These advances underscore the growing potential of rationally designed, strongly reducing organic photocatalysts in sustainable fluorine chemistry.

Inspired by this progress, we envisioned a new approach for constructing aza-heterocycles bearing difluoromethylene units via selective defluorination of trifluoromethylanilines. Our strategy involves photocatalytic single-electron reduction of trifluoromethylanilines to form radical anions, followed by fluoride elimination and intramolecular alkene difluoroalkylation. Herein, we report a mild and general method for the synthesis of difluoromethylene-containing aza-heterocycles, showcasing broad functional group tolerance and expanding the toolbox for C–F activation and heterocycle synthesis.

To evaluate our proposed strategy, we initiated studies on the intramolecular difluorocarbon hydrogenation of alkenes, selecting *ortho*-trifluoromethylaniline 1a as the model substrate for the synthesis of fluorinated tetrahydroquinolines.

**Received:** July 20, 2025

**Revised:** October 29, 2025

**Accepted:** November 17, 2025

**Published:** November 18, 2025



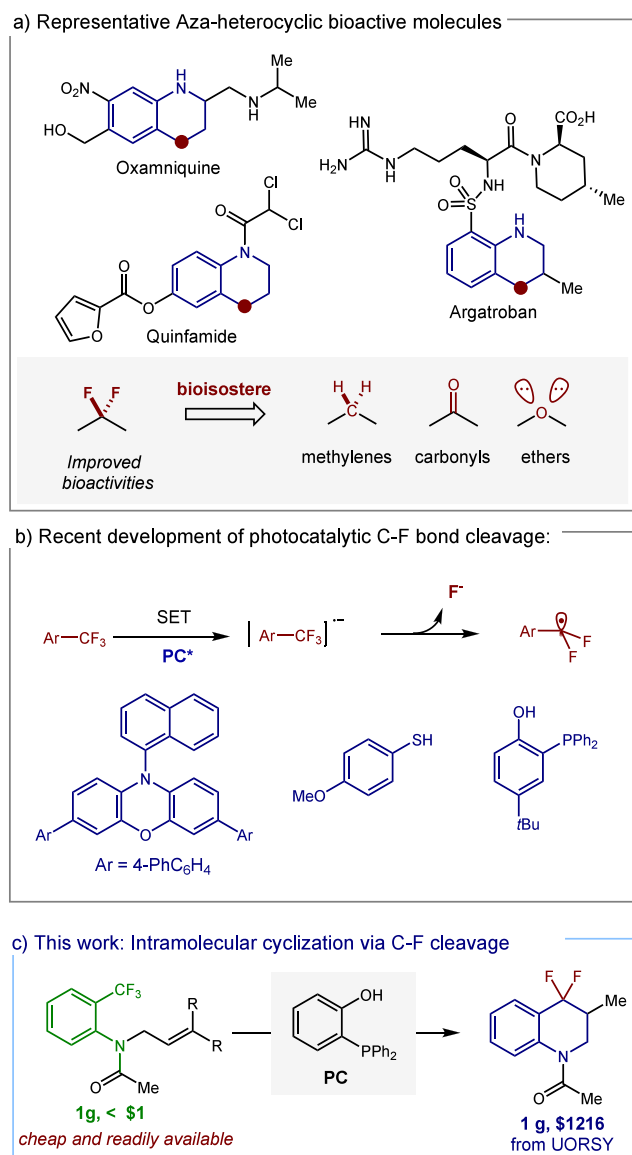
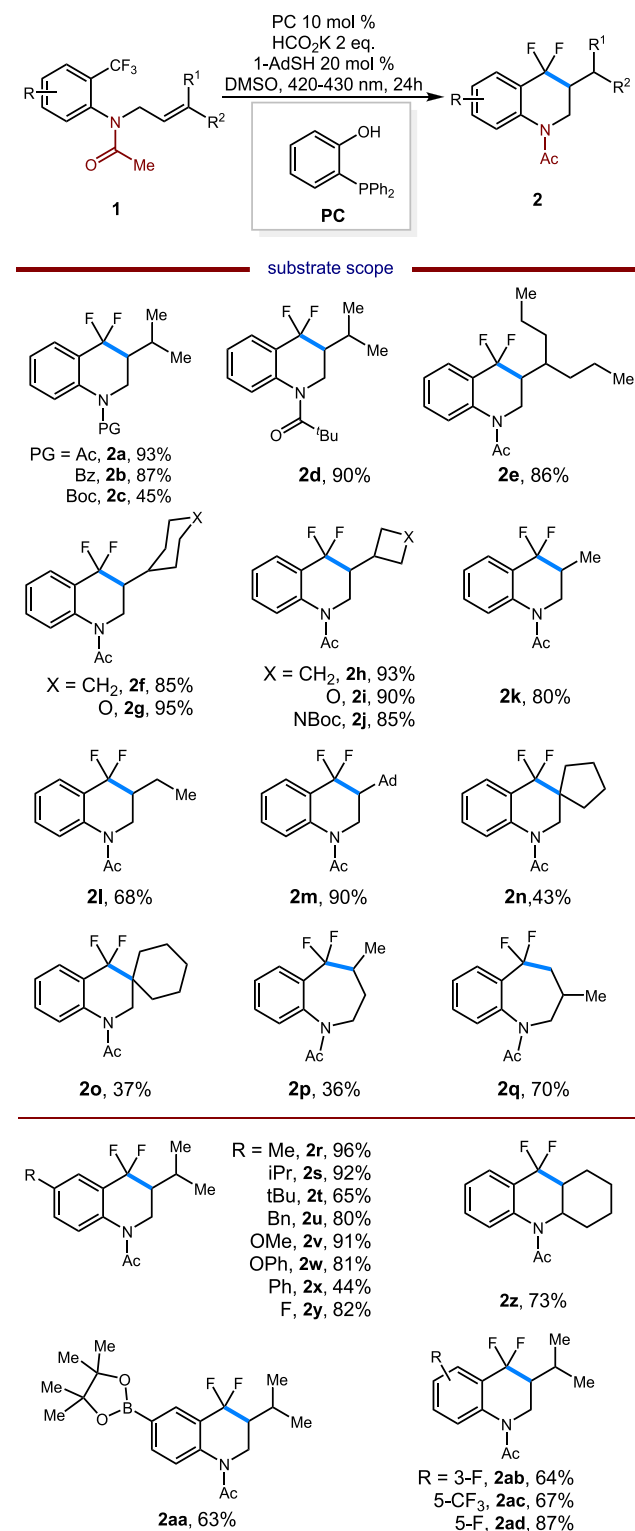


**Figure 1.** Background of selective defluorofunctionalization and reaction design.

Gratifyingly, under visible-light irradiation, the transformation proceeded efficiently with the organophotocatalyst developed by Shang and co-workers,<sup>16</sup> delivering **2a** in 93% yield under the optimized conditions: (2-hydroxyphenyl)-diphenylphosphine (photocatalyst), potassium formate ( $\text{HCO}_2\text{K}$ , reductant), 1-adamantanethiol (HAT catalyst), and DMSO as solvent under blue LED irradiation at ambient temperature (See detailed conditions optimization in SI). To systematically explore the generality of the selective defluorofunctionalization of trifluoromethylated anilines, we conducted substrate scope investigations under the optimized reaction conditions, as illustrated in Scheme 1. Initially, we assessed the impact of various N-protecting groups (Ac, Boc, Bz, and Pivaloyl) on substrate **1**. Remarkably, the reactions proceeded smoothly, yielding the corresponding products **2a–2d** in moderate to high yields, ranging from 45% to 93%.

Subsequently, a diverse array of alkenes was scrutinized in this transformation. Disubstituted alkenes of substrate **1** were well-tolerated, affording the desired products (**2e–2j**) in excellent yields, ranging from 85% to 95%. Terminal and

### Scheme 1. Substrate Scope<sup>a</sup>



<sup>a</sup>General conditions: **1** (0.2 mmol), Base (0.4 mmol), 1-AdSH (0.04 mmol), PC (0.02 mmol), DMSO (4.0 mL), blue LED (420–430 nm) with fan, rt,  $\text{N}_2$ , 24 h.

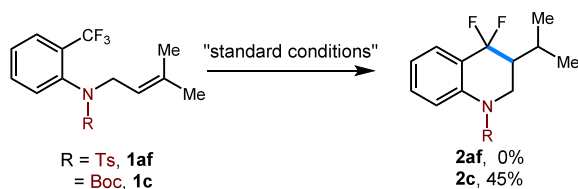
monosubstituted alkenes within substrate **1** were also amenable to the reaction, obtained the corresponding products **2k–2m** in good yields. Notably, cyclic olefins of substrate **1** demonstrated compatibility with this method, resulting in the formation of the expected products with moderate yields.

Specifically, a notable yield of **2p** was achieved via a 7-exo radical cyclization of **1p**, while a 7-endo radical cyclization of **1q** delivered **2q** in a 70% yield. Furthermore, we probed the influence of the electronic properties of the aromatic rings in substrate **1** on the reaction outcomes (Scheme 1). Introduction of electron-donating substituents such as alkyl groups and methoxyl/phenoxy groups onto the aromatic ring led to the formation of the corresponding products **2r–2y** in yields ranging from 44% to 96%. Notably, the lower yield of **2t** (65%) compared to **2s** (92%) is attributed to steric effects, as the bulkier *tert*-butyl group in **2t** likely restricts favorable substrate–photocatalyst orientations during the SET step, thereby increasing the SET barrier and reducing efficiency. Conversely, incorporation of electron-withdrawing substituents (as exemplified in Schemes 1, **1ab**, **1ac**, **1ad**) on the aromatic ring resulted in the synthesis of products **2ab** (64%), **2ac** (67%), and **2ad** (87%). Additionally, this strategy facilitated the synthesis of a tricyclic compound **2z** with a yield of 73%. The presence of a pinacolborane group on the aromatic ring was tolerated (**2aa**), broadening the scope of the reaction.

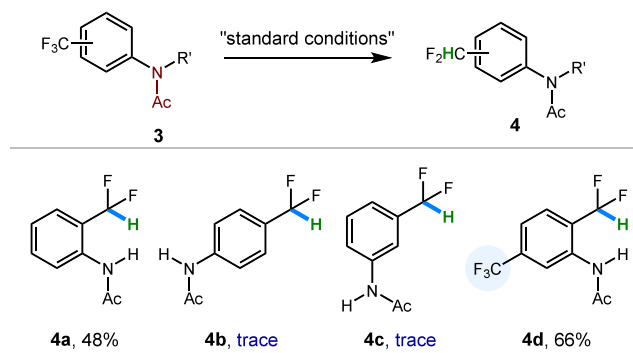
To investigate the influence of N-substitution on defluorohydrogenation reactivity (Scheme 2), we first examined a Ts-

### Scheme 2. Mechanistic Studies<sup>a</sup>

a) Influence of the N protecting group



b) The regioselectivity of defluorohydrogenation of trifluoromethylanilines



<sup>a</sup>General conditions: **1**/3 (0.2 mmol), Base (0.4 mmol), 1-AdSH (0.04 mmol), PC (0.02 mmol), DMSO (4.0 mL), blue LED (420–430 nm) with fan, rt, N<sub>2</sub>, 24 h.

protected trifluoromethylaniline (**1af**), which proved unreactive under standard conditions, likely due to unfavorable redox properties. In contrast, the NHAc-protected substrate **1c** afforded the desired product **2c** in 45% yield. Further evaluation of positional effects using *N*-phenylacetamide derivatives revealed that only the ortho-substituted trifluoromethylarene underwent productive defluorination (**4a**, 48%), while meta- and para-substituted analogs (**4b**, **4c**) remained unreactive. Notably, in a substrate bearing both ortho- and meta-CF<sub>3</sub> groups, defluorination occurred exclusively at the ortho position (**4d**, 66%), suggesting that regioselectivity is governed not solely by SET efficiency but also possible by

differential C–F bond cleavage kinetics. The ortho NHAc group may promote both electron transfer and facilitate C–F bond fragmentation, whereas distal CF<sub>3</sub> groups are more prone to unproductive back-electron transfer. To better understand these observations, we conducted computational studies to assess the electronic and energetic factors underlying this selectivity.

To elucidate the mechanistic origins of this regioselectivity, we performed thorough computational studies using the *w*B97X-D/6–311G(d,p) level of theory<sup>18</sup> with the SMD DMSO implicit solvent model.<sup>19</sup> Transition states and intermediates were optimized, and zero-point energy and free energy corrections were applied. The single-electron transfer (SET) was calculated using classical Marcus theory,<sup>20</sup> where the reorganizational energy ( $\lambda$ ) and free energy difference between the charge states ( $\Delta G_{SET}$ ) were calculated for each of the ortho, meta, and para isomers. The reaction follows a photocatalytic cycle in which the ground state photocatalyst (PC<sup>−</sup>) absorbs light and undergoes intersystem crossing to form a triplet species (TPC<sup>−</sup>). The SET reaction between TPC<sup>−</sup> and the trifluoromethyl substrate (**3**) results in the formation of an intermediate (**3'**), followed by a spin-center shift (SCS) to form the difluoromethyl intermediate (**3''**). The final hydrogen atom transfer (HAT) step from 1-AdSH regenerates the photocatalyst and furnishes the product (**4**). The overall reaction is highly exothermic, and each step (SET, SCS, and HAT) is associated with its own barrier. Among these, the SET step has the highest absolute barrier, while the HAT step shows the highest relative barrier. However, the SET step remains the rate-limiting process under our experimental conditions.<sup>21</sup> We calculated the excitation energy of the photocatalyst (PC<sup>−</sup>, T<sub>1</sub>) from its ground state (PC<sup>−</sup>, S<sub>0</sub>) to be 66.8 kcal·mol<sup>−1</sup>; although this plus the SET barrier represents the largest effective span, photoexcitation is efficient, making SET kinetically dominant.

The free energy profile in Figure 2 was generated after a comprehensive conformational search that explores the molecular complexes formed between the substrate and the photocatalyst. Approximately 190 conformers were generated and optimized using a multistep process involving MMFF force fields<sup>22</sup> and DFT reoptimization. The SET barriers were

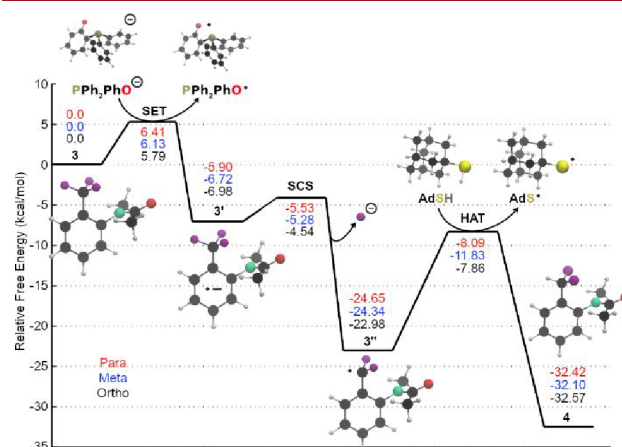


**Figure 2.** Free energy profile of the defluorohydrogenation reaction. The free energy profile of steps B, and C, and D are shown using classical Marcus theory for step B; ortho, meta, and para are shown in black, blue, and red, respectively. Example optimized geometries are shown for the ortho isomer.

calculated for the most stable complexes, with the ortho-isomer (black curve in Figure 2) displaying the lowest free energy barrier of 5.8 kcal/mol. This result supports the hypothesis that the SET step is the RLS. If the HAT step (blue curve in Figure 2) were the RLT, one would expect the meta-isomer to be the most reactive.

Further analysis of the electronic coupling ( $V_{AB}$ ) between the substrate and catalyst showed that the ortho isomer facilitated superior orbital overlap compared to the meta and para isomers. This was reflected in the dihedral angle scans (Figure 3), where the ortho-isomer exhibited a broader range

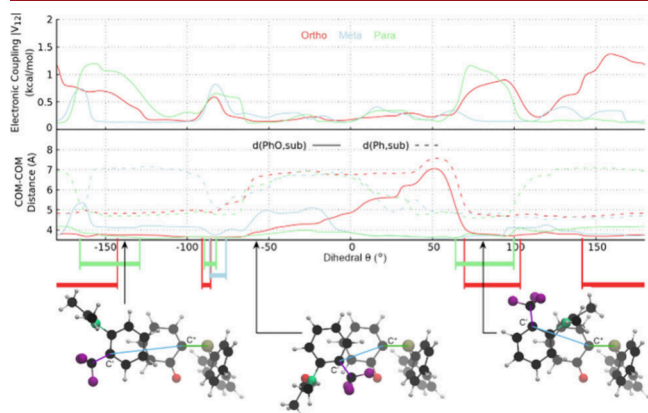


**Figure 3.** Free energy profiles for the ortho, meta, and para isomers. At top and center, the dihedral  $\theta$  defined as P-C\*-C'-CF<sub>3</sub>, is scanned, with example dihedrals of the optimized geometries shown at bottom. In the center, distances characterizing the closeness of PC<sup>-</sup> and 3 of the optimized geometries (described in main text) are plotted as a function of the dihedral. At the top, the electronic coupling is shown for the optimized geometries in kcal/mol. Relatively close distances between the catalyst and substrate as well as large electronic couplings are used to designate when an optimized substrate-catalyst geometry has an interaction, as shown by the colored bands (red for ortho, blue for meta, and green for para).

of geometries conducive to SET, contributing to its enhanced reactivity. The Boltzmann-weighted average rates for the SET reaction confirmed that the ortho isomer was the most reactive, with relative rates of 100:26:13 for the ortho, meta, and para species, respectively (Table S1).

It is important to note that while the dihedral scan analysis focused on one particular orientation of the 3/PC<sup>-</sup> molecular complex, other orientations were found as well in the full conformational search. As detailed in the SI, configurations roughly fell into four types as a result of different approaching directions of 3: “T1” conformers where 3 is close to and nearly parallel to the phenolate ring of PC<sup>-</sup>, “T2” conformers where 3 is instead parallel with the nonphenolate ring, “T3” conformers where 3 is in the opposite nonphenolate pocket altogether, and “T4” conformers where 3 is not in any particular pocket but is close to the PC<sup>-</sup>. However, of these, only the “T1” conformers have an “ideal” orientation of the molecules that are suspected to maximize the electronic coupling: i.e., where the donor HOMO on the PC<sup>-</sup> phenolate ring and the acceptor LUMO on the 3 phenyl ring would have maximal overlap (see Figures S1, S2).

In conclusion, through a combined experimental and computational study, we have demonstrated that the regioselectivity of trifluoromethylaniline defluorohydrogenation is strongly influenced by the substrate’s molecular

conformation and its interaction with the photocatalyst. The ortho-substituted species exhibits significantly higher reactivity due to favorable electronic coupling and low SET barriers, as confirmed by Marcus theory calculations. This study provides valuable insights into the design of selective defluorination reactions and highlights the potential for computational chemistry to predict and rationalize complex reaction mechanisms.

## ■ ASSOCIATED CONTENT

### Data Availability Statement

The data underlying this study are available in the published article and its Supporting Information.

### Supporting Information

The Supporting Information is available free of charge at <https://pubs.acs.org/doi/10.1021/acs.orglett.5c03024>.

Full experimental procedures, and spectroscopic data. (PDF)

## ■ AUTHOR INFORMATION

### Corresponding Authors

**Liejun Zhou** – Key Laboratory of the Ministry of Education for Advanced Catalysis Materials, College of Chemistry and Materials Science, Zhejiang Normal University, Jinhua 321004, P. R. China; [orcid.org/0000-0003-3929-2525](https://orcid.org/0000-0003-3929-2525); Email: [ljzhou@zjnu.cn](mailto:ljzhou@zjnu.cn)

**Rui Sun** – Department of Chemistry, University of Hawai‘i at Mānoa, Honolulu, Hawai‘i 96822, United States; [orcid.org/0000-0003-0638-1353](https://orcid.org/0000-0003-0638-1353); Email: [ruisun@hawaii.edu](mailto:ruisun@hawaii.edu)

**Zuxiao Zhang** – Department of Chemistry, University of Hawai‘i at Mānoa, Honolulu, Hawai‘i 96822, United States; [orcid.org/0000-0003-2365-6312](https://orcid.org/0000-0003-2365-6312); Email: [zzhang9@hawaii.edu](mailto:zzhang9@hawaii.edu)

### Authors

**Ting Long** – Key Laboratory of the Ministry of Education for Advanced Catalysis Materials, College of Chemistry and Materials Science, Zhejiang Normal University, Jinhua 321004, P. R. China

**Kazuomi Fujioka** – Department of Chemistry, University of Hawai‘i at Mānoa, Honolulu, Hawai‘i 96822, United States

**Yahui Wang** – Key Laboratory of the Ministry of Education for Advanced Catalysis Materials, College of Chemistry and Materials Science, Zhejiang Normal University, Jinhua 321004, P. R. China

**Qixin Zhou** – Key Laboratory of the Ministry of Education for Advanced Catalysis Materials, College of Chemistry and Materials Science, Zhejiang Normal University, Jinhua 321004, P. R. China

Complete contact information is available at: <https://pubs.acs.org/10.1021/acs.orglett.5c03024>

### Author Contributions

†T.L., K.F., and Y.W. contributed equally. The manuscript was written through contributions of all authors. All authors have given approval to the final version of the manuscript.

### Notes

The authors declare no competing financial interest.

## ACKNOWLEDGMENTS

This work is supported by the National Natural Science Foundation of China (22101258), the Leading Innovative and Entrepreneur Team Introduction Program of Zhejiang (No. 2022R01007) and the Start-up Research Grant from the Department of Chemistry, Zhejiang Normal University. The authors also appreciate the Information and Technology Services (ITS) from the University of Hawai'i, Manoa, and XSEDE for the computational resources.

## REFERENCES

- (1) Selected reviews: (a) Lovering, F.; Bikker, J.; Humblet, C. Escape from flatland: increasing saturation as an approach to improving clinical success. *J. Med. Chem.* **2009**, *52*, 6752. (b) Taylor, R. D.; MacCoss, M.; Lawson, A. D. Rings in drugs. *J. Med. Chem.* **2014**, *57*, 5845. (c) Vitaku, E.; Smith, D. T.; Njardarson, J. T. Analysis of the structural diversity, substitution patterns, and frequency of nitrogen heterocycles among U.S. FDA approved pharmaceuticals. *J. Med. Chem.* **2014**, *57*, 10257. (d) Schneider, N.; Lowe, D. M.; Sayle, R. A.; Tarselli, M. A.; Landrum, G. A. Big data from pharmaceutical patents: a computational analysis of medicinal chemists' bread and butter. *J. Med. Chem.* **2016**, *59*, 4385. (e) Candeias, N. R.; Branco, L. C.; Gois, P. M. P.; Afonso, C. A. M.; Trindade, A. F. More Sustainable Approaches for the Synthesis of N-Based Heterocycles. *Chem. Rev.* **2009**, *109*, 2703. (f) Gao, B.; Yang, B.; Feng, X.; Li, C. Recent advances in the biosynthesis strategies of nitrogen heterocyclic natural products. *Nat. Prod. Rep.* **2022**, *39*, 139.
- (2) Danso-Appiah, A.; Olliaro, P. L.; Donegan, S.; Sinclair, D.; Utzinger, J. Drugs for treating *Schistosoma mansoni* infection. *Cochrane Database Syst. Rev.* **2019**, *2*, DOI: 10.1002/14651858.CD000528.pub2.
- (3) Dixon, M.; Lien, H. Tolvaptan and its potential in the treatment of hyponatremia. *Ther. Clin. Risk Manag.* **2008**, *4*, 1149.
- (4) McKeage, K.; Plosker, G. L. *Argatroban*. *Drugs* **2001**, *61*, 515.
- (5) Importance of aliphatic organofluorine compounds, see: (a) Jeschke, P. The Unique Role of Fluorine in the Design of Active Ingredients for Modern Crop Protection. *ChemBioChem.* **2004**, *5*, 570. (b) Purser, S.; Moore, P. R.; Swallow, S.; Gouverneur, V. Fluorine in medicinal chemistry. *Chem. Soc. Rev.* **2008**, *37*, 320. (c) Hagmann, W. K. The Many Roles for Fluorine in Medicinal Chemistry. *J. Med. Chem.* **2008**, *51*, 4359. (d) Gillis, E. P.; Eastman, K. J.; Hill, M. D.; Donnelly, D. J.; Meanwell, N. A. Applications of Fluorine in Medicinal Chemistry. *J. Med. Chem.* **2015**, *58*, 8315. (e) Zhou, Y.; Wang, J.; Gu, Z.-N.; Wang, S.-N.; Zhu, W.; Aceña, J. L.; Soloshonok, V. A.; Izawa, K.; Liu, H. Next Generation of Fluorine-Containing Pharmaceuticals Compounds Currently in Phase II–III Clinical Trials of Major Pharmaceutical Companies: New Structural Trends and Therapeutic Areas. *Chem. Rev.* **2016**, *116*, 422.
- (6) (a) Tozer, M. J.; Herpin, T. F. Methods for the synthesis of gem-difluoromethylene compounds. *Tetrahedron* **1996**, *52*, 8619. (b) Landelle, G.; Panossian, A.; Pazenok, S.; Vors, J.-P.; Leroux, F. R. Recent advances in transition metal-catalyzed Csp<sup>2</sup>-monofluoro-, difluoro-, perfluoromethylation and trifluoromethylthiolation. *Beilstein J. Org. Chem.* **2013**, *9*, 2476. (c) Zhao, Y.; Ni, C.; Jiang, F.; Gao, B.; Shen, X.; Hu, J. Copper-Catalyzed Debenzyloxylation of Monofluoromethylation of Aryl Iodides Assisted by the Removable (2-Pyridyl)sulfonyl Group. *ACS Catal.* **2013**, *3*, 631. (d) Yudin, A. K.; Prakash, G. K. S.; Deffieux, D.; Bradley, M.; Bau, R.; Olah, G. A. Preparation of and Fluoroalkylation with (Chlorodifluoromethyl)Trimethylsilane, Difluorobis(trimethylsilyl)-Methane, and 1,1,2,2-Tetrafluoro-1,2-Bis(trimethylsilyl)Ethane. *J. Am. Chem. Soc.* **1997**, *119*, 1572. (e) Meanwell, N. A. Synopsis of Some Recent Tactical Application of Bioisosteres in Drug Design. *J. Med. Chem.* **2011**, *54*, 2529. (f) Erickson, J. A.; McLoughlin, J. I. Hydrogen Bond Donor Properties of the Difluoromethyl Group. *J. Org. Chem.* **1995**, *60*, 1626. (g) Lu, Y.; Liu, C.; Chen, Q.-Y. Recent Advances in Difluoromethylation Reaction. *Curr. Org. Chem.* **2015**, *19*, 1638. (h) Sessler, C. D.; Rahm, M.; Becker, S.; Goldberg, J. M.; Wang, F.; Lippard, S. J. CF<sub>2</sub>H, a Hydrogen Bond Donor. *J. Am. Chem. Soc.* **2017**, *139*, 9325. (i) Yerien, D. E.; Barata-Vallejo, S.; Postigo, A. Difluoromethylation Reactions of Organic Compounds. *Chem. - Eur. J.* **2017**, *23*, 14676. (j) Rong, J.; Ni, C.-F.; Hu, J.-B. Metal-Catalyzed Direct Difluoromethylation Reactions. *Asian J. Org. Chem.* **2017**, *6*, 139.
- (7) (a) Wright, S. E.; Bandar, J. S. A Base-Promoted Reductive Coupling Platform for the Divergent Defluorofunctionalization of Trifluoromethylarenes. *J. Am. Chem. Soc.* **2022**, *144*, 13032. (b) Mandal, D.; Gupta, R.; Jaiswal, A. K.; Young, R. D. Frustrated Lewis-Pair-Mediated Selective Single Fluoride Substitution in Trifluoromethyl Groups. *J. Am. Chem. Soc.* **2020**, *142*, 2572. (c) Luo, C.; Bandar, J. S. Selective Defluoroallylation of Trifluoromethylarenes. *J. Am. Chem. Soc.* **2019**, *141*, 14120. (d) Idogawa, R.; Kim, Y.; Shimomori, K.; Hosoya, T.; Yoshida, S. Single C–F Transformations of *o*-Hydroxysilyl Benzotrifluorides with Trityl Compounds as All-in-One Reagents. *Org. Lett.* **2020**, *22*, 9292. (e) Xiao, R.; Lang, Y.; Cheng, Z.; Zhou, L.; Cao, Z.-Y.; Yuan, Z.; Wang, Y. Decatungstate-Catalyzed Hydroxylation of  $\alpha$ -Trifluoromethylalkenes for Construction of  $\alpha$ -Trifluoromethyl- $\beta$ -silanes. *Org. Lett.* **2025**, *27*, 4439.
- (8) (a) Andrieux, C. P.; Combellas, C.; Kanoufi, F.; Savéant, J. M.; Thiébaud, A. Dynamics of Bond Breaking in Ion Radicals. Mechanisms and Reactivity in the Reductive Cleavage of Carbon-Fluorine Bonds of Fluoromethylarenes. *J. Am. Chem. Soc.* **1997**, *119*, 9527. (b) Box, J. R.; Avanthay, M. E.; Poole, D. L.; Lennox, A. J. J. Electronically Ambivalent Hydrodefluorination of Aryl-CF<sub>3</sub> Groups Enabled by Electrochemical Deep-Reduction on a Ni Cathode. *Angew. Chem., Int. Ed.* **2023**, *62*, No. e202218195.
- (9) (a) Fujita, T.; Fuchibe, K.; Ichikawa, J. Transition-Metal-Mediated and -Catalyzed C–F Bond Activation by Fluorine Elimination. *Angew. Chem., Int. Ed.* **2019**, *58*, 390. (b) Kraft, B. M.; Lachicotte, R. J.; Jones, W. D. Aliphatic Carbon–Fluorine Bond Activation Using (C<sub>5</sub>Me<sub>5</sub>)<sub>2</sub>ZrH<sub>2</sub>. *J. Am. Chem. Soc.* **2000**, *122*, 8559. (c) Kraft, B. M.; Jones, W. D. Mechanism of Vinylic and Allylic Carbon–Fluorine Bond Activation of Non-Perfluorinated Olefins Using Cp\*<sub>2</sub>ZrH<sub>2</sub>. *J. Am. Chem. Soc.* **2002**, *124*, 8681.
- (10) (a) Caputo, C. B.; Stephan, D. W. Activation of Alkyl C–F Bonds by B(C<sub>6</sub>F<sub>5</sub>)<sub>3</sub>: Stoichiometric and Catalytic Transformations. *Organometallics* **2012**, *31*, 27. (b) Mandal, D.; Gupta, R.; Young, R. D. Selective Monodefluorination and Wittig Functionalization of gem-Difluoromethyl Groups to Generate Monofluoroalkenes. *J. Am. Chem. Soc.* **2018**, *140*, 10682. (c) Mandal, D.; Gupta, R.; Jaiswal, A. K.; Young, R. D. Frustrated Lewis-Pair-Mediated Selective Single Fluoride Substitution in Trifluoromethyl Groups. *J. Am. Chem. Soc.* **2020**, *142*, 2572. (d) Lye, K.; Young, R. D. A review of frustrated Lewis pair enabled monoselective C–F bond activation. *Chem. Sci.* **2024**, *15*, 2712.
- (11) (a) Andrieux, C. P.; Combellas, C.; Kanoufi, F.; Savéant, J.; Thiébaud, A. Dynamics of Bond Breaking in Ion Radicals. Mechanisms and Reactivity in the Reductive Cleavage of Carbon–Fluorine Bonds of Fluoromethylarenes. *J. Am. Chem. Soc.* **1997**, *119*, 9527. (b) Clavel, P.; Lessene, G.; Biran, C.; Bordeau, M.; Roques, N.; Trevin, S.; de Montauzon, D. Selective electrochemical synthesis and reactivity of functional benzylic fluorosilyl synthons. *J. Fluorine Chem.* **2001**, *107*, 301. (c) O'Hagan, D. Understanding organofluorine chemistry. An introduction to the C–F bond. *Chem. Soc. Rev.* **2008**, *37*, 308. (d) Coleman, J. P.; Gilde, H. G.; Utley, J. H. P.; Weedon, B. C. L. The electrochemical reductive cleavage of carbon–oxygen and carbon–fluorine bonds in benzylic systems. *J. Chem. Soc. D* **1970**, *0*, 738.
- (12) Chen, K.; Berg, N.; Gschwind, R.; König, B. Selective Single C(sp<sup>3</sup>)-F Bond Cleavage in Trifluoromethylarenes: Merging Visible-Light Catalysis with Lewis Acid Activation. *J. Am. Chem. Soc.* **2017**, *139*, 18444.
- (13) (a) Wang, H.-B.; Jui, N. Catalytic Defluoroalkylation of Trifluoromethylaromatics with Unactivated Alkenes. *J. Am. Chem. Soc.* **2018**, *140*, 163. (b) Vogt, D.; Seath, C.; Wang, H.-B.; Jui, N. Selective

C–F Functionalization of Unactivated Trifluoromethylarenes. *J. Am. Chem. Soc.* **2019**, *141*, 13203.

(14) Sap, J.; Straathof, N.; Knauber, T.; Meyer, C.; Médebielle, M.; Buglioni, L.; Genicot, C.; Trabanco, A.; Noël, T.; am Ende, C.; Gouverneur, V. *J. Am. Chem. Soc.* **2020**, *142*, 9181.

(15) (a) Luo, C.; Bandar, J. S. Selective Defluoroallylation of Trifluoromethylarenes. *J. Am. Chem. Soc.* **2019**, *141*, 14120.

(b) Sugihara, N.; Suzuki, K.; Nishimoto, Y.; Yasuda, M. Photo-redox-Catalyzed C–F Bond Allylation of Perfluoroalkylarenes at the Benzylic Position. *J. Am. Chem. Soc.* **2021**, *143*, 9308. (c) Ai, H.-J.; Ma, X.-X.; Song, Q.-L.; Wu, X.-F. C-F Bond Activation under Transition-Metal-Free Conditions. *Sci. China Chem.* **2021**, *64*, 1630.

(d) Luo, Y.-C.; Tong, F.-F.; Zhang, Y.; He, C.-Y.; Zhang, X. Visible-Light-Induced Palladium-Catalyzed Selective Defluoroarylation of Trifluoromethylarenes with Arylboronic Acids. *J. Am. Chem. Soc.* **2021**, *143*, 13971. (e) Wang, J.; Wang, Y.; Liang, Y.; Zhou, L.; Liu, L.; Zhang, Z. Late-Stage Modification of Drugs via Alkene Formal Insertion into Benzylic C-F Bond. *Angew. Chem., Int. Ed.* **2023**, *62*, No. e202215062.

(16) (a) Liu, C.; Shen, N.; Shang, R. Photocatalytic defluoroalkylation and hydrodefluorination of trifluoromethyls using *o*-phosphinophenolate. *Nat. Commun.* **2022**, *13*, 354. (b) Liu, C.; Li, K.; Shang, R. Arenethiolate as a Dual Function Catalyst for Photocatalytic Defluoroalkylation and Hydrodefluorination of Trifluoromethyls. *ACS Catal.* **2022**, *12*, 4103–4109. (c) Liu, C.; Shen, N.; Shang, R. Photocatalytic Defluoroalkylation of Trifluoroacetates with Alkenes using 4-(Acetamido)thiophenol. *Synthesis* **2023**, *55*, 1401. (d) Shen, N.; Li, R.; Liu, C.; Shen, X.; Guan, W.; Shang, R. Photocatalytic Cross-Couplings of Aryl Halides Enabled by *o*-Phosphinophenolate and *o*-Phosphinothiophenolate. *ACS Catal.* **2022**, *12*, 2788.

(17) Liu, C.; Zhang, Y.; Shang, R. BINOLates as Strongly Reducing Photocatalysts for Inert Bond Activation and Reduction of Unsaturated Systems. *Chem.* **2025**, *11*, 102359.

(18) (a) Chai, J. D.; Head-Gordon, M. Systematic optimization of long-range corrected hybrid density functionals. *J. Chem. Phys.* **2008**, *128*, 8. (b) Krishnan, R.; Binkley, J. S.; Seeger, R.; Pople, J. A. Self-consistent molecular orbital methods. XX. A basis set for correlated wave functions. *J. Chem. Phys.* **1980**, *72*, 650. (c) Francl, M. M.; Pietro, W. J.; Hehre, W. J.; Binkley, J. S.; Gordon, M. S.; DeFrees, D. J.; Pople, J. A. Self-consistent molecular orbital methods. XXIII. A polarization-type basis set for second-row elements. *J. Chem. Phys.* **1982**, *77*, 3654. (d) McLean, A. D.; Chandler, G. S. Contracted Gaussian basis sets for molecular calculations. I. Second row atoms, Z= 11–18. *J. Chem. Phys.* **1980**, *72*, 5639.

(19) (a) Miertuš, S.; Scrocco, E.; Tomasi, J. Electrostatic interaction of a solute with a continuum. A direct utilization of AB initio molecular potentials for the prevision of solvent effects. *Chem. Phys.* **1981**, *55*, 117. (b) Cossi, M.; Barone, V.; Cammi, R.; Tomasi, J. Ab initio study of solvated molecules: a new implementation of the polarizable continuum model. *Chem. Phys. Lett.* **1996**, *255*, 327.

(20) (a) Marcus, R. A.; Sutin, N. Electron transfers in chemistry and biology. *Biochim Biophys Acta Bioenerg* **1985**, *811*, 265. (b) Marcus, R. A. Electron transfer reactions in chemistry: theory and experiment (Nobel lecture). *Angew Chem Int Ed* **1993**, *32*, 1111. (c) Newton, M. D. Quantum chemical probes of electron-transfer kinetics: the nature of donor-acceptor interactions. *Chem Rev.* **1991**, *91*, 767.

(21) Murdoch, J. R. What is the rate-limiting step of a multistep reaction? *J. Chem. Educ.* **1981**, *58*, 32.

(22) Halgren, T. A. Merck molecular force field. I. Basis, form, scope, parameterization, and performance of MMFF94. *J. Comput. Chem.* **1996**, *17*, 490.